

## EVOLUTION OF THE PHASE-SPACE DENSITY IN DARK MATTER HALOS

YEHUDA HOFFMAN<sup>1</sup>, EMILIO ROMANO-DÍAZ<sup>2</sup>, ISAAC SHLOSMAN<sup>2</sup>, CLAYTON HELLER<sup>3</sup>

*Accepted for publication by the Astrophysical Journal*

### ABSTRACT

The evolution of the phase-space density profile in dark matter (DM) halos is investigated by means of constrained simulations, designed to control the merging history of a given DM halo. Halos evolve through a series of quiescent phases of a slow accretion intermitted by violent events of major mergers. In the quiescent phases the density of the halo closely follows the NFW profile and the phase-space density profile,  $Q(r)$ , is given by the Taylor & Navarro power law,  $r^{-\beta}$ , where  $\beta \approx 1.9$  and stays remarkably stable over the Hubble time. Expressing the phase-space density by the NFW parameters,  $Q(r) = Q_s(r/R_s)^{-\beta}$ , the evolution of  $Q$  is determined by  $Q_s$ . We have found that the effective mass surface density within  $R_s$ ,  $\Sigma_s \equiv \rho_s R_s$ , remains constant throughout the evolution of a given DM halo along the main branch of its merging tree. This invariance entails that  $Q_s \propto R_s^{-5/2}$  and  $Q(r) \propto \Sigma_s^{-1/2} R_s^{-5/2} (r/R_s)^{-\beta}$ . It follows that the phase-space density remains constant, in the sense of  $Q_s = \text{const.}$ , in the quiescent phases and it decreases as  $R_s^{-5/2}$  in the violent ones. The physical origin of the NFW density profile and the phase-space density power law is still unknown. Yet, the numerical experiments show that halos recover these relations after the violent phases. The major mergers drive  $R_s$  to increase and  $Q_s$  to decrease discontinuously while keeping  $Q_s \times R_s^{5/2} = \text{const.}$  The virial equilibrium in the quiescent phases implies that a DM halos evolves along a sequence of NFW profiles with constant energy per unit volume (i.e., pressure) within  $R_s$ .

*Subject headings:* cosmology: dark matter — galaxies: evolution — galaxies: formation — galaxies: halos — galaxies: interactions — galaxies: kinematics and dynamics

### 1. INTRODUCTION

The dynamics of dark matter (DM) halos in the Cold Dark Matter (CDM) cosmology can be easily formulated as the classical Newtonian  $N$ -body problem. Yet, the understanding of the equilibrium configuration of the DM halos defies a simple analytical approach. The lack of analytical understanding is often compensated for by numerical simulations which provide empirical knowledge. The cumulative work in cosmology over the last decade or so has led to a broad consensus about two basic facts that describe the equilibrium structure of DM halos. One is that the spherically-averaged density profile  $\rho(r)$  is well approximated by the so-called NFW profile (Navarro et al. 1996, 1997) or some close variants of it (Moore et al. 1998; Jing & Suto 2000; Klypin et al. 2001). The other is the power law behavior of the phase-space density profile, namely  $Q(r) = \rho(r)/\sigma^3(r) \propto r^{-\beta}$ , with  $\beta \approx 1.9$ , where  $\sigma(r)$  is the velocity dispersion (Taylor & Navarro 2001).

Two seemingly orthogonal approaches to the problem of the origin of the equilibrium structure in DM halos exist. One assumes a monolithic collapse of a halo that can be approximated by the spherical infall model (Gunn & Gott 1972). The application of the model to the cosmological context, where the shell crossing has to be explicitly accounted for, has resulted in the so-called secondary

infall model (SIM; Gunn 1977; Fillmore & Goldreich 1984; Bertschinger 1985; Hoffman & Shaham 1985; Ryden & Gunn 1987; Zaroubi & Hoffman 1993; Nusser 2001; Lokas & Hoffman 2000). The SIM has been tested against the  $N$ -body simulations and has proven to faithfully reproduce the density profile of simulated DM halos (Quinn et al. 1986; Efstathiou et al. 1988; Crone et al. 1994; Ascasibar et al. 2004; 2007). A closely related variant of the SIM replaces its dependence on the primordial over-density of the proto-halo by the mass accretion history (MAH) of the halo (Nusser & Sheth 1999; Lu et al. 2006; Salvador-Solé et al. 2007). The SIM and its MAH variant can reproduce also the power law behavior of the phase-space density (Austin et al. 2005; González-Casado et al. 2007).

However, a close inspection of the  $N$ -body simulations reveals that a DM halo evolves very differently from a monolithic quasi-spherical collapse. In fact halos are numerically observed to go through a sequence of mergers, some labeled as major mergers in which the two main progenitors are of a similar mass, leading to emergence of the NFW density profile (Syer & White 1998; Dekel et al. 2003; Subramanian et al. 2000). Romano-Diaz et al. (2006; 2007, hereafter Paper I and II) studied the formation and equilibrium configuration of halos by means of controlled  $N$ -body simulations, with the initial conditions set by constrained realizations of Gaussian fields. These simulations were designed to address issues of how the merging history affects the DM halos. The emerging picture is that of a halo evolving *via* a sequence of quiescent phases of a slow mass accretion intermitted by violent episodes of major mergers. In the quiescent phases, the

<sup>1</sup> Racah Institute of Physics, Hebrew University; Jerusalem 91904, Israel

<sup>2</sup> Department of Physics and Astronomy, University of Kentucky, Lexington, KY 40506-0055, USA

<sup>3</sup> Department of Physics, Georgia Southern University, Statesboro, GA 30460, USA

density is well fitted by an NFW profile, the inner (NFW) scale radius  $R_s$  and the mass enclosed within it ( $M_s$ ) remain constant, and the virial radius ( $R_{\text{vir}}$ ) grows linearly with the expansion parameter ( $a$ ). In the violent phases, the halos are not in a dynamical equilibrium, but are rather in a transition state, resulting in a discontinuous growth of  $R_s$  and  $R_{\text{vir}}$ . In such a picture a halo is defined in the context of a merger tree — at any given time it is taken as the most massive progenitor along the branch leading to the final halo.

A direct comparison between the SIM and numerical simulations has been conducted recently by Ascasibar et al. (2007). This comparison is based on selecting the DM halos from a cosmological simulation, tracing them back in time, and recovering their individual initial conditions. The SIM has been applied to the ‘primordial’ density profiles, and their virial density profiles have been calculated for different redshifts. The SIM calculated profiles provided a good match to the evolution and structure of the simulated clusters. This is encouraging. However, a rigorous fundamental theory that can accommodate both the spherical monolithic collapse and the major merger-driven evolution exhibited by the simulations is still missing. This motivates us to look further into the phenomenology of the phase-space density, to gain a further insight into this seemingly simple, yet complicated, problem.

The study of the DM halo evolution has been heavily focused on the density profile, while the evolution of the phase-space density has been largely ignored. Peirani & de Freitas Pacheco (2007) presented one of the few studies of  $Q(r)$  evolution. They found that  $Q$ , defined as a global quantity characterizing the halo as a whole, is generally decreasing with time. Specifically, it exhibits an early rapid decrease (at redshifts  $z \gtrsim 6.5$ ) and a late slow decrease. Here we aim at studying the evolution of the phase-space density within the framework of the NFW scaling and the dynamical picture formulated in Papers I and II. In particular, we shall rely on the empirical fact that the dynamics of the DM halos is constrained by a new invariant of motion. This invariant tags a halo along the main branch of the merging tree. The NFW scaling and this invariant of motion provide a full description of the cosmological evolution of the phase-space density for individual halos.

The structure of the paper is as follows. The analysis of the DM halos in Papers I and II is briefly reviewed in §2. General considerations of the evolution of DM halos are given in §3. The general evolution of the DM phase-space density profile is described in §4 and self-similarity and scaling relations are given in §5. A general discussion follows in §6.

## 2. NUMERICAL EXPERIMENTS

In Papers I and II, we investigated the cosmological evolution and structure of five DM halos by setting the initial conditions of the simulations using constrained realizations of Gaussian fields. Our basic motivation was to perform controlled numerical experiments designed to study the dependence of the evolution and structure of a given halo on its merging history. The Hoffman & Ribak (1991) algorithm of constrained realizations of Gaussian fields has been used to set up the initial conditions. Papers I and II present the analysis of five different mod-

els of a given DM halo, evolving along various merging histories. The models were simulated within the framework of the open CDM (OCDM) model with  $\Omega_0 = 0.3$ ,  $h = 0.7$  and  $\sigma_8 = 0.9$ , where  $\Omega_0$  is the current cosmological matter density parameter and  $\sigma_8$  is the variance of the density field convolved with a top-hat window of radius  $8h^{-1}\text{Mpc}$  used to normalize the power spectrum. This model is very close to the ‘concordance’  $\Lambda\text{CDM}$  model in its dynamical properties. The models are labeled as OCDMa, OCDMb, etc., following the notations of Papers I and II. Here we add a new model, run within the flat- $\Lambda$  cosmology with the parameters of the WMAP three years data base (Spergel et al. 2006). The constraints used to set the model are similar to OCDMa and the model is labeled as WMAP3a, yet it is performed within a  $256^3$  computational box and it starts from a different random realization of the initial conditions. A full description of the numerical simulations, the application of the algorithm of constrained realizations and the numerical code are given in Papers I and II. The WMAP3a model is one in a series of runs in the WMAP3 cosmology, to be reported in a forthcoming paper. The NFW fitting algorithm is described in Paper II and the phase-space density power law profile is fitted in a similar way.

## 3. GENERAL CONSIDERATIONS

The density profile of DM halos is well approximated by the NFW profile,

$$\rho(r) = \frac{4\rho_s}{(r/R_s)(1+r/R_s)^2}, \quad (1)$$

in which the characteristic density ( $\rho_s$ ) and scale radius ( $R_s$ ) define the NFW profile. Defining the halo as a collection of particles in a spherical (say) volume in which the mean density equals some critical over-density (which is in general redshift dependent) times the mean cosmological density, the virial mass ( $M_{\text{vir}}$ ) and radius ( $R_{\text{vir}}$ ) of the halo are determined. It follows that  $R_{\text{vir}}$  and  $R_s$  (or equivalently  $M_{\text{vir}}$  and  $M_s$ ) are the two independent parameters that define an NFW halo.

Assuming the NFW parameterization, we can write the phase-space density profile as

$$Q(r) = Q_s \mathcal{Q}\left(\frac{r}{R_s}\right), \quad (2)$$

where

$$\mathcal{Q}(x) = \frac{\rho(x)/\rho_s}{[\sigma(x)/\sigma_s]^3}, \quad (3)$$

$$Q_s = \frac{\rho_s}{\sigma_s^3}, \quad (4)$$

$\sigma_s$  is the mean velocity dispersion within  $R_s$  and  $x = r/R_s$ . To the extent that the DM halos are fitted by the NFW profile, their  $\mathcal{Q}(x)$  profile should obey a universal relation. Their cosmological evolution is then determined by the evolution of  $Q_s$ .

## 4. EVOLUTION OF DARK MATTER HALOS

The cosmological evolution of the main halo of the six different models is best presented by Fig. 1, which shows the evolution of  $R_s$  and  $Q_s$ . The halo goes through violent episodes of major mergers and quiescent phases of slow accretion. In the OCDM models the violent events

are well separated by the quiescent phases characterized by an NFW structure (Papers I and II). The WMAP3 model goes through an early phase of successive violent mergers, frequent enough so that the halo does not relax to an NFW-like configuration in between. This early phase is followed by a quiescent phase, which is slightly perturbed by mergers not strong enough to be qualified as major. This is clearly shown by the behavior  $R_s$  and  $Q_s$ , where  $R_s$  ( $Q_s$ ) increases (decreases) discontinuously in the violent phases and remains constant in the quiescent ones. One should note that in the violent episodes the halos are not in an equilibrium and therefore the NFW fitting is very unstable and the resulting  $R_s$  and  $Q_s$  parameters are quite erratic. This is reflected by the spiky behavior of these quantities in the violent phases.

Evolution of the dimensionless phase-space density profile,  $\mathcal{Q}(x)$ , is presented in Fig. 2, where the  $\mathcal{Q}(r/R_s)$  profiles of the  $\Lambda$ CDM and WMAP3 models are evaluated at different epochs, covering the time interval from  $z = 5.3$  ( $z = 3.35$ ) for the  $\Lambda$ CDM (WMA3) model to the present epoch. The evolution of the other models is virtually identical to the ones shown here. The  $\mathcal{Q}(x)$  profiles are very closely approximated by a power law, with a fractional deviation of less than a twenty percent (lower panel of Fig. 2). Fig. 2 shows not only the power law nature of the profiles but also that indeed the  $Q_s$  scaling renders the  $\mathcal{Q}(x)$  profile to a universal time independent power law. The evolution of the exponents of the  $\mathcal{Q}(x)$  fitted power law of all the models is shown in Fig. 3.  $\beta$  displays a bumpy behavior, with bumps corresponding to the major mergers, but generally staying within the  $\beta \approx 1.9 \pm 0.1$  range. Overall, given the violent character of the halo's evolution, the robustness of the  $\beta$  range is remarkable.

A close inspection of the halo evolution reveals that the product  $\Sigma_s \equiv \rho_s R_s$  remains approximately invariant as the halo evolves along the main branch of its merging tree (Fig. 4). The value of  $\Sigma_s$  fluctuates around its mean value in two different modes.. undergoes fast and correlated fluctuations of a small amplitude (see next section and Paper II). In the violent episodes it exhibits large deviations from the mean value. This behavior is associated with timings of major mergers when halos are far from the equilibrium. The NFW fitting fails here and the resulting NFW parameters are ill-defined. Ignoring the spikes of the violent phases, and averaging over the jittery fluctuations in the quiescent phases,  $\Sigma_s$  retains its value along the halo evolution. *While the invariance of  $\Sigma_s$  in a given quiescent phase is not surprising, its ability to retain the value in and across the major merger events is not obviously expected.*

## 5. SELF-SIMILARITY AND SCALING RELATIONS

Assuming the empirical finding of  $\Sigma_s$  invariance, we shall study its ramifications for the evolution of the phase-space density. In the quiescent phases, in which the density follows the NFW profile, a halo is expected to be in virial equilibrium, as corroborated by Fig. 13 of Paper II. In particular the virial ratio, evaluated within  $R_s$ , should have a constant value, namely,

$$\frac{\sigma_s^2}{M_s/R_s} \approx const. \quad (5)$$

The virial ratio differs from unity because the inner part of the halo does not constitute an isolated system, and its value depends on the shape of the density profile.

Assuming the constancy of the virial ratio within  $R_s$  and the invariance of  $\Sigma_s$ ,

$$\sigma_s^2 \rho_s \propto \frac{M_s \rho_s}{R_s} \propto \rho_s^2 R_s^2 = \Sigma_s^2. \quad (6)$$

The evolution of the phase-space density profile in a given halo is described by

$$Q(r) \propto \Sigma_s^{-1/2} R_s^{-5/2} \left( \frac{r}{R_s} \right)^{-\beta}. \quad (7)$$

Consequently, for a given halo the following invariance holds:

$$Q_s R_s^{5/2} \approx const. \quad (8)$$

This prediction has been tested against the five models of Papers I and II and the  $\Lambda$ CDM halo. Fig. 5 shows the cosmological evolution of  $Q_s R_s^{5/2}$  of these models. As with all other quantities that characterize the DM halos, the product  $Q_s R_s^{5/2}$  shows a jittery behavior in the quiescent phases and strong fluctuations in the violent phases, in which the NFW parameters are ill defined. Apart from this, it remains constant throughout the evolution. Only Model C exhibits a small deviation from this invariance. In its first quiescent phase  $Q_s R_s^{5/2}$  is larger by a factor of  $\lesssim 1.5$  than its asymptotic value.

The  $\rho_s R_s$  invariance is to be distinguished from the  $\rho_s \propto R_s^{-m}$  scaling found in its the low-amplitude jitter (Paper II) and from  $M_s \propto R_s^\alpha$  of Zhao et al. (2003). In Paper II we show that  $m \approx 1.39$  in the last quiescent phases of various halos, while at early times  $m \approx 1.59$ . This stands in good agreement with Zhao et al.'s  $\alpha \approx 1.44$  in the ‘‘slow accretion phase’’ and  $\alpha \approx 1.92$  in the ‘‘rapid accretion phase.’’ The  $m \approx 1.39$  scaling is obtained by analyzing each quiescent phase, and it reflects the fluctuations of  $\rho_s$  and  $R_s$  around their mean values within that phase. This correlation appear to be driven by density fluctuations that originate in the region between the cusp and  $R_s$ , where the density slope varies between -1 and -2. The mean values of  $\rho_s$  and  $R_s$  change from one quiescent phase to another. The  $m \approx 1.59$  reflects the variation across the different phases. The association of the  $m \approx 1.59$  and  $\alpha \approx 1.92$  with the early times of the evolution of halos stems from the fact that the violent phases are more abundant at early times. The combined analysis of Paper II and the present work yields the following picture. In the quiescent phases the values of  $\rho_s$  and  $R_s$  fluctuate around constant values, yet their product remains invariant along the evolution of a halo.

The  $\Sigma_s$  invariance implies that  $M_s \propto R_s^2$ . This is very close to the  $M_s \propto R_s^{1.92}$  of Zhao et al. (2003) and the minor discrepancy results from Zhao et al. not separating explicitly between the quiescent and violent phases. We, therefore, support and validate one of Zhao et al.'s main points, namely the  $M_s \propto R_s^\alpha$  scaling, and set  $\alpha = 2$ . Thus, we validate also Zhao et al.'s relation between the evolution of the concentration parameter and the MAH. Moreover, this relation can be easily extended to the MAH —  $Q_s$  relation, given the  $Q_s R_s^{5/2}$  invariance.

A final note concerns the entropy of a system of self-gravitating collisionless particles. The definition of the

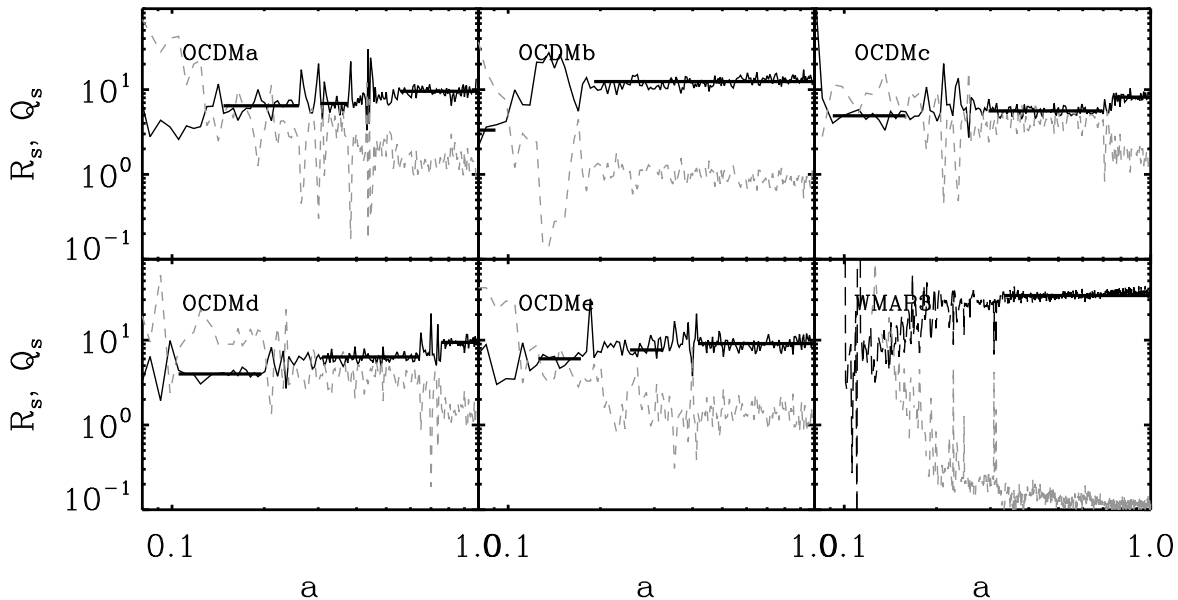


FIG. 1.— The cosmological evolution of the main halo of the six models is shown as a function of the expansion parameter  $a$ . The violent phases are characterized by sudden increase (decrease) of  $R_s$ , indicated by continuous lines, ( $Q_s$ , dashed lines) and these quantities remain roughly constant in the quiescent phase. At the violent phases the NFW fitting fails and the resulting  $R_s$  and  $Q_s$  become unstable. The thick horizontal lines correspond to the mean value of  $R_s$  within the different quiescent phases. The WMAP3 model exhibits an extended initial phase of a succession of violent mergers that cannot be resolved into individual ones separated by quiescent phases, like in the OCDM models. This is followed by a quiescent phase. The  $Q_s$  curves have been shifted to fit within the window.

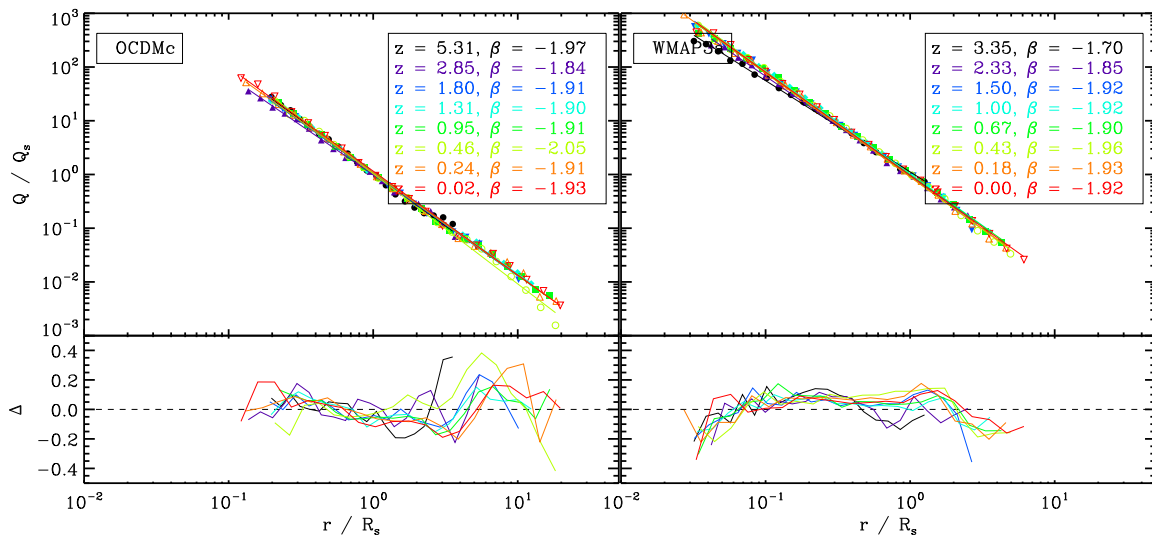


FIG. 2.— The cosmological evolution of the dimensionless phase-space density profile,  $Q(r/R_s)$ , of the OCDMc (left panel) and the  $\Lambda$ CDM WMAP3a (right panel) halos. The  $Q(r/R_s)$  profile is plotted for a sample of snapshots for the two halos. The value of  $\beta$  for each snapshot is indicated. The bottom panels show the fractional residual deviation from a power law. The relative deviation from a power law behavior is smaller than twenty percent. The universal form of  $Q(r/R_s)$  is clearly exhibited. The  $Q(r/R_s)$  profiles of the other OCDM models are virtually identical to the ones shown here.

entropy (per particle) of a monoatomic ideal gas is given by

$$s = k_B \ln(Q^{-1}) + const, \quad (9)$$

where  $k_B$  is the Boltzmann constant (*e.g.*, Dalcanton & Hogan 2001; White & Narayan 1987). Applying this definition to the DM particles provides one with a formal entropy of the DM. Our findings concerning structure and evolution of the phase-space density can be easily translated to the language of the entropy of the DM. It should be noted here that Eq.

9 provides a local measure of the entropy. The long range nature of the gravitational interactions prohibits a simple extension of the entropy to an extensive quantity that characterizes the whole halo. Within this framework we can only refer to the entropy as a local property.

## 6. DISCUSSION AND CONCLUSIONS

The main elements of the structure and evolution of the DM halos can be summarized as follows. Halos evolve through two phases, quiescent and violent ones, which

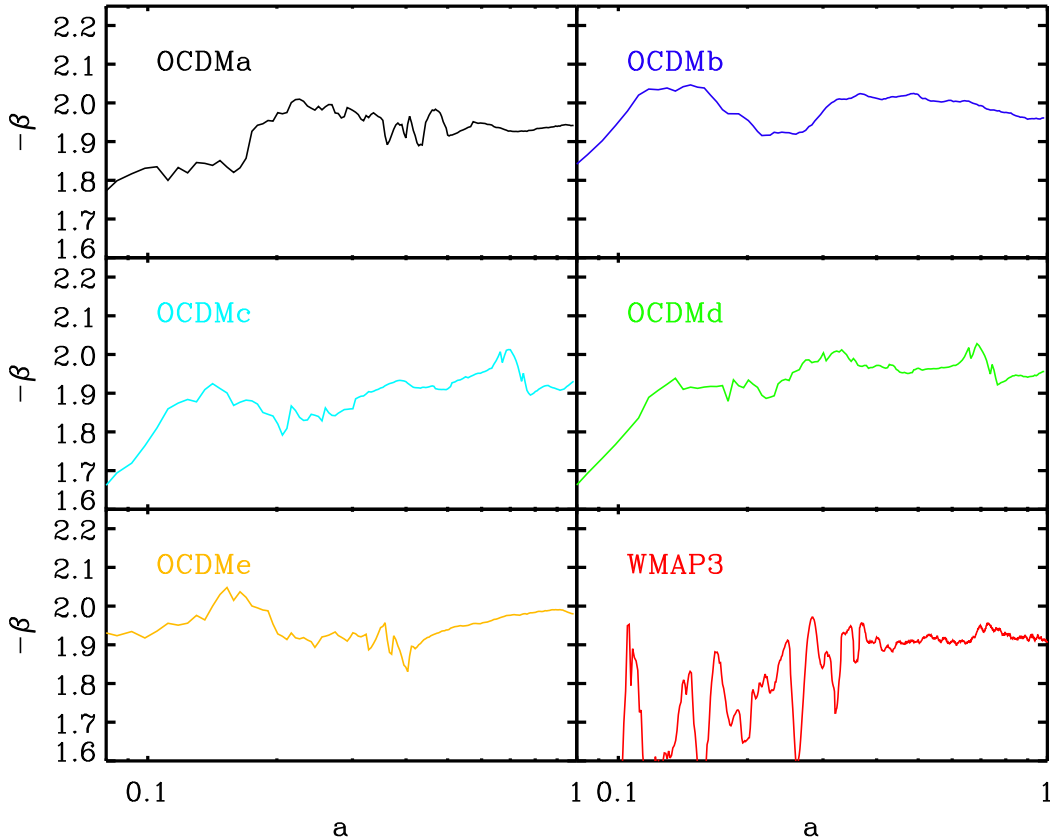


FIG. 3.— The evolution of the slope of the phase-space density power law ( $\beta$ ) is plotted against the expansion parameter  $a$  for the six halo models.

represent the two extreme cases of smooth accretion and major mergers. In the quiescent phase the halo density distribution is closely approximated by the NFW profile. The inner (within  $R_s$ ) halo mass surface density,  $\Sigma_s$ , remains approximately constant throughout its entire evolution. Most importantly, the major mergers that take the halo from one quiescent phase to the other preserve the value of  $\Sigma_s$ . During the quiescent phases the halo phase-space density profile follows a power law of the form  $Q(r) = Q_s(r/R_s)^{-\beta}$  with  $\beta \approx 1.9$ . The cosmological evolution of the phase space density is given by  $Q_s$ . Under the invariance of  $\Sigma_s$  and the assumption of the virial equilibrium within  $R_s$ , the evolution of  $Q_s$  is dictated by  $R_s$ , so that  $Q_s \propto R_s^{-5/2}$ . In the quiescent phases,  $Q_s$  remains constant and it decreases discontinuously in the violent phases.

The  $\Sigma_s$  invariance and the virial theorem (Eq. 6) imply that the evolution of a halo proceeds while conserving its surface density and its energy per unit volume, or equivalently the pressure, within  $R_s$ . The interesting point is that a typical halo undergoes a few violent events of major merging that destroy its equilibrium. Following each event it regains the NFW structure with a larger  $R_s$ , while preserving its pressure and the mean surface density within the new  $R_s$ . Summarizing, a DM halo evolves along a sequence of NFW profiles, with an ever increasing  $R_{vir}$  and  $R_s$  that grows only discontinuously,

in the manner described in Paper I, while conserving the mean surface density and the pressure within  $R_s$ .

The evolution of the  $Q(r)$  profile of a given DM halo is predicted by Eq. 7. The controlled numerical experiments of Papers I and II suggest that, for a given halo,  $\Sigma_s$  remains constant over a few quiescent phases intermitted by violent events. All the halos analyzed here (apart from WMAP3a) emerge from the same realization of the initial conditions that has been subjected to different constraints. In many ways these halos can be considered as a single halo that has been manipulated so as to modify its merging history. As such they all have roughly the same value of  $\Sigma_s$ . The WMAP3a model provides an independent realization of a DM halo in a different cosmology. The value of  $\Sigma_s$  is roughly twice as large than in all the other model. Of course the extremely poor statistics of our models cannot teach us about the scatter in  $\Sigma_s$ . The question arises as to what happens in the general case of a large ensemble of DM halos drawn from a large cosmological simulation. The scatter in  $\Sigma_s$  is expected to determine the evolutionary tracks of the phase-space density profiles. It is interesting to study the possible environment  $-\Sigma_s$  correlation, and to what extent this affects the evolution of the DM halos.

The  $\rho_s R_s$  invariance implies that the Zhao et al. (2003)  $M_s \propto R_s^\alpha$  scaling holds with  $\alpha = 2$ , and so does the MAH - concentration parameter relation. It follows that this

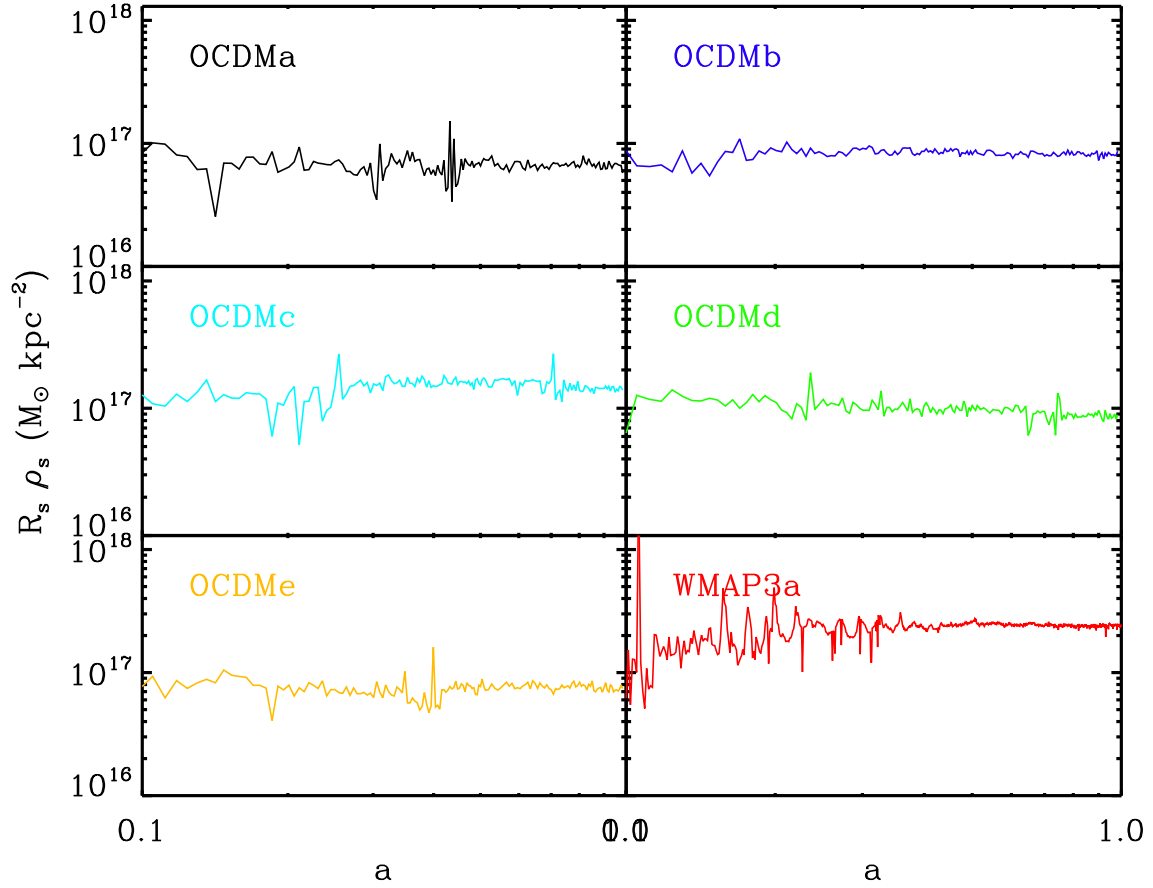


FIG. 4.— The product  $\Sigma_s = \rho_s R_s$  is plotted against the expansion parameter  $a$  for the six halo models. The panels present the individual models.  $\Sigma_s$  exhibits a jittery behavior in the quiescent phases and the large spikes correspond to the violent epochs in which the NFW fitting is ill-defined. Apart from these,  $\Sigma_s$  remains approximately constant throughout the evolution.

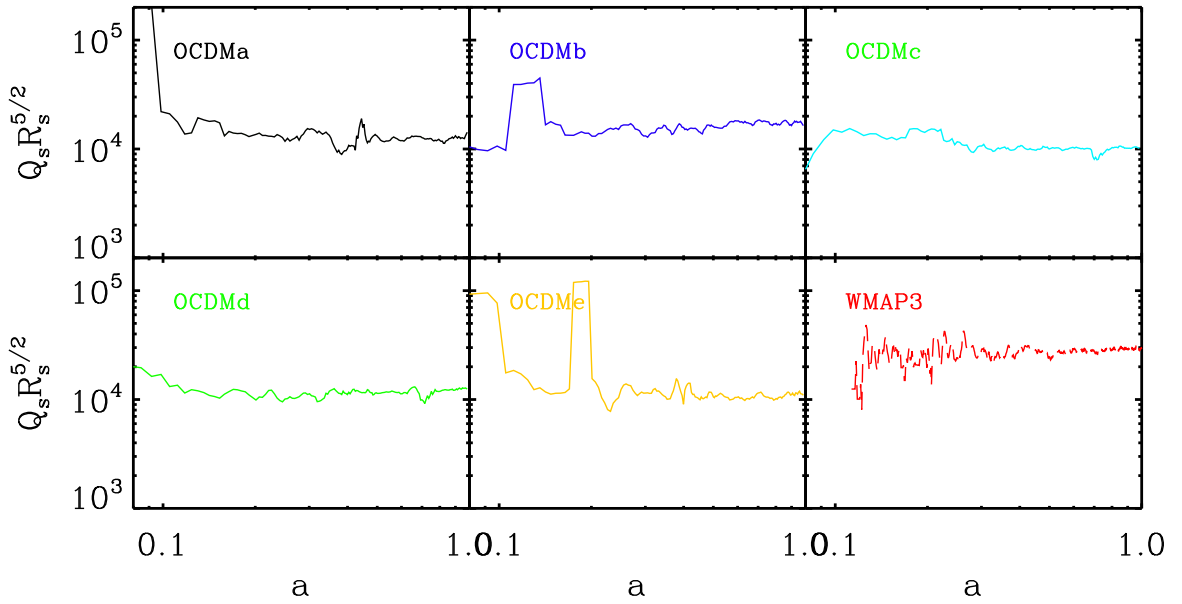


FIG. 5.— The cosmological evolution  $Q_s R_s^{5/2}$  of the main halo of the six models is shown as a function of the expansion parameter  $a$ .  $Q_s R_s^{5/2}$  behaves very similarly to  $\Sigma_s$  (Fig. 4).

can be easily extended to calculate a similar MAH  $-Q_s$  relation. The interesting ramification of this result is

that any statistical algorithm for generating DM halos merging trees and/or MAHs can be extended so as to provide the evolution of the full NFW parameters of a halo along its merging tree. This can be used in semi-analytical modeling of galaxy formation in which realizations of merging trees include the full NFW structure of the halos.

The definition of  $Q(r)$  as a phase-space density is only a poor man's substitute for the 'real' phase-space density in the six-dimensional phase space. Yet, pushing the analogy further on, a formal entropy is defined by Eq. 9 as a local variable. This local definition cannot be extended to provide a global entropy of the halo. It follows that statements regarding the evolution of the entropy of DM halos are ill-defined, at least in the current context. Nevertheless, in the NFW scaling framework, in which the entropy of DM halos is taken as  $Q_s$ , it increases with  $R_s$ . In this context, the quiescent phases with  $R_s \sim \text{const.}$  correspond to adiabatic processes which preserve the entropy, and the violent phases — to non-adiabatic ones in which the entropy grows.

The method of introducing an entropy by means of Eq. 9 can be considered as only formal, and its relation to a standard thermodynamics needs to be questioned. Yet, Faltenbacher et al. (2007) have recently shown that the formally defined entropy of the DM is very closely associated with the classical (ideal gas) entropy of the intergalactic gas in clusters of galaxies. Faltenbacher et al. studied the entropy of the gas and DM in high resolution adiabatic SPH cosmological simulations — 'adiabatic' here is used in the sense that the entropy of the gas can only grow due to shock waves. Consequently,

following the accepted notation, the entropy of the gas can be expressed by means of  $K_{gas} \equiv k_B T / \rho^{2/3}$ , and by analogy  $K_{DM} = \sigma_{DM}^2 / \rho_{DM}^{2/3} \propto Q^{-2/3}$ . The power law behavior of  $Q(r)$  implies that  $K_{DM} \propto r^{1.1}$ . Interestingly, outside the entropy core of  $r \approx R_s/2$  the gas entropy follows the DM, namely  $K_{gas} \propto K_{DM}$ , and the calculated slope agrees well with observations. Faltenbacher *et al.* amended the definition of  $K_{gas}$ , such that the thermal energy is extended to include the kinetic energy of the small scale (turbulent motion) and the DM and gas densities are normalized by their mean cosmological values. The newly defined  $K_{gas}$  then coincides with the DM entropy outside the entropy core to a very good approximation. The analysis of Faltenbacher *et al.* shows that, at least in galaxy clusters, the DM entropy coincides with the classical, ideal gas, entropy of the intracluster medium. It is not clear a priori why the gas and DM entropies should coincide, but numerical simulations suggest that they do. The simulations suggest that observational determination of the entropy of the intracluster gas should shed light and constrain the behavior of the DM entropy.

We thank Ran Rubin for his help with the calculation of the phase space density profile. Fruitful discussions with Yuval Birnboim, Adi Nusser, Noam Soker and Saleem Zaroubi are gratefully acknowledged. This research has been supported by ISF-143/02 and the Sheinborn Foundation (to YH), by NASA/LTSA 5-13063, NASA/ATP NAG5-10823, HST/AR-10284 (to IS), and by NSF/AST 02-06251 (to CH and IS).

## REFERENCES

- Ascasibar, Y., Hoffman, Y., & Gottlöber, S. 2007, Monthly Notices of the Royal Astronomical Society, 376, 393
- Ascasibar, Y., Yepes, G., Gottlöber, S., & Müller, V. 2004, MNRAS, 352, 1109
- Austin, C. G., Williams, L. L. R., Barnes, E. I., Babul, A., & Dalcanton, J. J. 2005, ApJ, 634, 756
- Bertschinger, E. 1985, ApJS, 58, 39
- Crone, M. M., Evrard, A. E., & Richstone, D. O. 1994, ApJ, 434, 402
- Dalcanton, J. J. & Hogan, C. J. 2001, ApJ, 561, 35
- Dekel, A., Arad, I., Devor, J., & Birnboim, Y. 2003, ApJ, 588, 680
- Efstathiou, G., Frenk, C. S., White, S. D. M., & Davis, M. 1988, MNRAS, 235, 715
- Faltenbacher, A., Hoffman, Y., Gottlöber, S., & Yepes, G. 2007, MNRAS, 376, 1327
- Fillmore, J. A. & Goldreich, P. 1984, ApJ, 281, 1
- González-Casado, G., Salvador-Solé, E., Manrique, A., & Hansen, S. H. 2007, ArXiv Astrophysics e-prints
- Gunn, J. E. 1977, ApJ, 218, 592
- Gunn, J. E. & Gott, J. R. I. 1972, ApJ, 176, 1
- Hoffman, Y. & Ribak, E. 1991, ApJ, 380, L5
- Hoffman, Y. & Shaham, J. 1985, ApJ, 297, 16
- Jing, Y. P. & Suto, Y. 2000, ApJ, 529, L69
- Klypin, A., Kravtsov, A. V., Bullock, J. S., & Primack, J. R. 2001, ApJ, 554, 903
- Lokas, E. L. & Hoffman, Y. 2000, ApJ, 542, L139
- Lu, Y., Mo, H. J., Katz, N., & Weinberg, M. D. 2006, MNRAS, 401
- Moore, B., Governato, F., Quinn, T., Stadel, J., & Lake, G. 1998, ApJ, 499, L5+
- Navarro, J. F., Frenk, C. S., & White, S. D. M. 1996, ApJ, 462, 563
- . 1997, ApJ, 490, 493
- Nusser, A. 2001, MNRAS, 325, 1397
- Nusser, A. & Sheth, R. K. 1999, MNRAS, 303, 685
- Peirani, S. & de Freitas Pacheco, J. A. 2007
- Quinn, P. J., Salmon, J. K., & Zurek, W. H. 1986, Nature, 322, 329
- Romano-Díaz, E., Faltenbacher, A., Jones, D., Heller, C., Hoffman, Y., & Shlosman, I. 2006, ApJ, 637, L93
- Romano-Díaz, E., Hoffman, Y., Heller, C., Faltenbacher, A., Jones, D., & Shlosman, I. 2007, ApJ, 657, 56
- Ryden, B. S. & Gunn, J. E. 1987, ApJ, 318, 15
- Salvador-Solé, E., Manrique, A., González-Casado, G., & Hansen, S. H. 2007, ArXiv Astrophysics e-prints
- Spergel, D. N., Bean, R., Doré, O., Nolta, M. R., Bennett, C. L., Dunkley, J., Hinshaw, G., Jarosik, N., Komatsu, E., Page, L., Peiris, H. V., Verde, L., Halpern, M., Hill, R. S., Kogut, A., Limon, M., Meyer, S. S., Odegard, N., Tucker, G. S., Weiland, J. L., Wollack, E., & Wright, E. L. 2006, ArXiv Astrophysics e-prints
- Subramanian, K., Cen, R., & Ostriker, J. P. 2000, ApJ, 538, 528
- Syer, D. & White, S. D. M. 1998, MNRAS, 293, 337
- Taylor, J. E. & Navarro, J. F. 2001, ApJ, 563, 483
- White, S. D. M. & Narayan, R. 1987, MNRAS, 229, 103
- Zaroubi, S. & Hoffman, Y. 1993, ApJ, 416, 410
- Zhao, D. H., Mo, H. J., Jing, Y. P., & Börner, G. 2003, MNRAS, 339, 12